Letter | Editors' Suggestion

Sublattice interference promotes pair density wave order in kagome metals

Yi-Ming Wu,[1] Ronny Thomale,[2,3] and S. Raghu[1]

[1]*Stanford Institute for Theoretical Physics, Stanford University, Stanford, California 94305, USA*

[2]*Institute for Theoretical Physics and Astrophysics, University of Würzburg, D-97074 Würzburg, Germany*

[3]*Department of Physics and Quantum Centers in Diamond and Emerging Materials (QuCenDiEM) Group, Indian Institute of Technology Madras, Chennai 600036, India*

(Received 17 November 2022; revised 2 August 2023; accepted 7 August 2023; published 22 August 2023)

Motivated by the observation of a pair density wave (PDW) in the kagome metal CsV_3Sb_5, we consider the fate of electrons near a p-type Van Hove singularity (vHS) of the kagome lattice with on-site Hubbard U and the nearest-neighbor repulsion V. We study the effect of such interactions on Fermi surface "patches" at the vHS. We show how a feature unique to the kagome lattice known as sublattice interference crucially affects the form of the interactions among the patches. The renormalization group (RG) flow of such interactions results in a regime where the nearest-neighbor interaction V exceeds the on-site repulsion U. We identify this condition as being favorable for the formation of charge-density-wave (CDW) and PDW orders. In the weak-coupling limit, we find a complex CDW order as the leading instability, which breaks time-reversal symmetry. Beyond RG, we perform a Hartree-Fock study to a V-only model and find the pair-density-wave order indeed sets in at some intermediate coupling.

DOI: 10.1103/PhysRevB.108.L081117

Introduction. Spins and electrons on the kagome lattice [Fig. 1(a)] have long been studied due to their potential for exhibiting a panoply of exotic phases of matter. Insulating kagome compounds, for instance, are among the most prominent candidate spin liquid materials [1], and insulating phases with nontrivial topology have also been studied on the kagome lattice [2–4]. With the discovery of a family of kagome metals AV_3Sb_5 (A = K, Cs, Rb), a new wave of excitement has been elicited by the prospects for intriguing density wave and superconducting ground states in these systems [5–7].

Among the more fascinating observed phenomena in these kagome metals include new Bragg-like peaks inside the superconducting phase [8], a hallmark of an exotic superconducting order known as a pair density wave (PDW) [9–24] PDWs are superconductors with an order parameter that varies periodically in space. Additionally, fascinating effects have been discovered in the superconducting fluctuation spectrum, including nearly condensed excited states with charge 4e, 6e superconducting fluctuations [25]. These observations call for a greater theoretical scrutiny, and invite us to make predictions for electronic phases of kagome metals.

In this Letter, motivated by these recent developments, we address the issue of whether the PDW superconducting phase can in principle arise on the kagome lattice. Since such superconductivity requires analysis of the intermediate coupling problem, robust pairing mechanisms for PDW formation have only recently been uncovered [26]. One key requirement for PDW order is the presence of strong-repulsive interactions with somewhat suppressed on-site interactions. While this is rather unusual in most solids, we show here that this requirement is met when the chemical potential crosses a so-called p-type (for "pure") Van Hove singularity (vHS) [27–30] [see Fig. 1(b)]. In an important theoretical study, one of us showed [27] that precisely at such a p-type vHS, there is the phenomena of sublattice interference (SI)—where each of the three distinct sublattices has nonzero support only on *one* of the three distinct vH points. To show this SI crucially determines the low-energy effective interactions in the system, we construct a renormalization group (RG) theory based on the p-type vHS and show that the on-site repulsion runs towards weak coupling, while nearest-neighbor interactions grow under the RG. This peculiarity results in a rich phase diagram including time-reversal symmetry breaking charge-density-wave (CDW) orders and various uniform superconductivity in the weak-coupling limit; while in the strong-coupling regime it makes the kagome system poised to exhibit the PDW order. While more experiments are needed to characterize precisely the normal state in this system, our analysis already establishes that the kagome motif once again provides us with an avenue towards an exotic phase of matter, in this case the PDW superconductor.

SI and the triviality of Hubbard U. To determine the fate of effective interactions at p-type Van Hove filling, we utilize parquet RG methods and restrict attention to Fermi surface "patches" in the neighborhood of the distinct Van Hove points [31,32] (similar RG analysis with twofold of Van Hove singularities is considered in Ref. [33]). Defining the fermion destruction operators in patch α as ψ_α, we encode real-space 4-fermion interactions as intra- and interpatch couplings after Fourier transformation. In a crystal with time-reversal and/or inversion symmetry, such interactions take the form $H_I = g_1\psi_\alpha^\dagger\psi_\beta^\dagger\psi_\alpha\psi_\beta + g_2\psi_\alpha^\dagger\psi_\beta^\dagger\psi_\beta\psi_\alpha + g_3\psi_\alpha^\dagger\psi_\alpha^\dagger\psi_\beta\psi_\beta + g_4\psi_\alpha^\dagger\psi_\alpha^\dagger\psi_\alpha\psi_\alpha$ where $\alpha \neq \beta$ and the momentum summation and a spin configuration $\sigma\sigma'\sigma'\sigma$ is assumed. Patch models have been applied to the square lattice [34], the honeycomb lattice [35,36], and moiré systems [21,37,38]

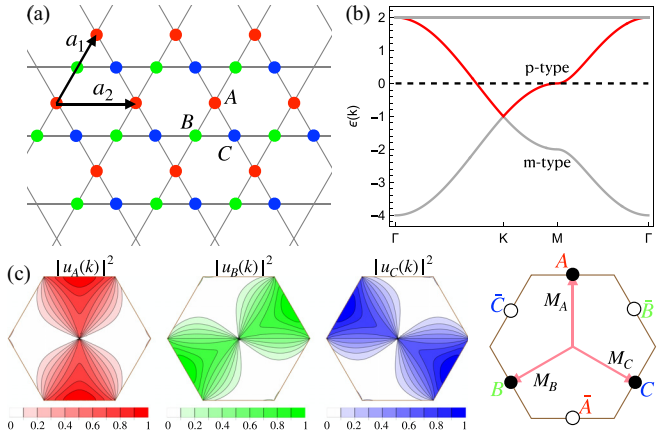

FIG. 1. Sublattice interference in the kagome lattice. (a) Each unit cell has $\alpha =$ A, B, C different sublattice sites. (b) Band structure of the tight-binding model. We focus on the middle band, highlighted with red color, which exhibits a p-type Van Hove singularity. (c) For this band, the transformation matrix $u_\alpha(\boldsymbol{k})$, defined as $c_\alpha(\boldsymbol{k}) = u_\alpha(\boldsymbol{k})\psi_\alpha(\boldsymbol{k})$ where c_α and ψ_α are lattice and band fermions respectively, has a modulated distribution in the Brillouin zone.

to capture interaction-driven electronic orders. In both cases, *all* the g_i's are set by the largest Hubbard on-site interaction $H_U = U\sum_i n_{i\uparrow}n_{i\downarrow}$.

However, adopting the same strategy on the kagome lattice near a p-type vHS, one finds that the Hubbard interaction U contributes only to the g_4. This is due to SI: Near a p-type vHS, each of the three sublattices (A,B,C) has nonzero support only on *one* of the three distinct Van Hove points ($\boldsymbol{M}_\alpha, \alpha = A, B, C$), which is visible through the sublattice weight in Fig. 1(c). The SI does not result from fine tuning, as it exists even if longer range hoppings are considered [39]. Thus, when only H_U is present for electrons near a p-type vHS, $g_1 = g_2 = g_3 = 0$, and $g_4 = U/t$. With this choice of bare couplings, g_4 weakens under RG flow, eventually reaching a trivial fixed point with $g_4^* = 0$ [39]. Thus, due to SI, the repulsive Hubbard U is irrelevant in the RG sense near the p-type vHS of the kagome lattice[40].

Extended interactions and the six-patch theory. Due to the apparent irrelevance of U, it is necessary to include at least nearest-neighbor interactions. The most important such term is the nearest-neighbor density-density repulsion $H_V = V\sum_{\langle ij\rangle} n_i n_j$. With both H_U and H_V, the three-patch model described above is no longer adequate since nearest-neighbor interactions contain momentum dependence, which differentiates the patches at $\pm\boldsymbol{M}_\alpha$. Therefore, we need to consider the full six-patch theory, for which there are 16 different symmetry allowed interactions in total, as shown in Fig. 2(a). Here we adopt the convention used in Ref. [37] and define the patch fermions as $\psi_{\alpha+} = \psi(\boldsymbol{k} \to \boldsymbol{M}_\alpha)$ and $\psi_{\alpha-} = \psi(\boldsymbol{k} \to -\boldsymbol{M}_\alpha)$. The interactions in this six-patch model can be written as

$$H_I = \sum_{i,j=1}^{4}\sum_{\{\alpha_j,\tau_j\}} g_{ij}\psi^\dagger_{\alpha_1\tau_1}\psi^\dagger_{\alpha_2\tau_2}\psi_{\alpha_3\tau_3}\psi_{\alpha_4\tau_4}, \qquad (1)$$

with g_{ij} being the dimensionless interaction strengths. Momentum conservation constrains the indices as follows: The patch indices satisfy $\alpha_1 = \alpha_3 \neq \alpha_2 = \alpha_4$ for $i = 1$, $\alpha_1 = \alpha_4 \neq \alpha_2 = \alpha_3$ for $i = 2$, $\alpha_1 = \alpha_2 \neq \alpha_3 = \alpha_4$ for $i = 3$, and $\alpha_1 = \alpha_2 = \alpha_3 = \alpha_4$ for $i = 4$. The "valley" indices $\tau_i = \pm$, labeling whether the patch is at $\boldsymbol{M}_\alpha$ or $-\boldsymbol{M}_\alpha$, obey the same rule associated with j. That is, $\tau_1 = \tau_3 \neq \tau_2 = \tau_4$ for $j = 1$, et cetera. Once again, SI crucially influences the initial conditions of the RG flows. A straightforward calculation [39] shows that U contributes only to g_{4j}—a direct generalization of the three-patch theory—while V only contributes to g_{2j},

$$g_{4j,0} = \frac{U}{t}; g_{22,0} = g_{24,0} = -g_{21,0} = -g_{23,0} = \frac{2V}{t}. \qquad (2)$$

The subscript 0 above denotes bare interactions before running RG. From microscopics, it is natural to expect that U (and therefore $g_{4j,0}$) should be the largest.

CDW at weak coupling. We first investigate the weak-coupling limit. In this case the fate of the fermions can be described by the one loop RG equations of g_{ij}, for which we keep the most divergent "log squared" terms in perturbation theory, i.e., the particle-hole bubble $\Pi^{(0)}_{ph}$ at momenta $\boldsymbol{M}_\alpha$ and the particle-particle bubble $\Pi^{(0)}_{pp}$ at zero momentum, and set the running parameter as the latter: $y = \Pi^{(0)}_{pp}(0)$ [37,39]. With this convention, the RG equations for the interactions take the

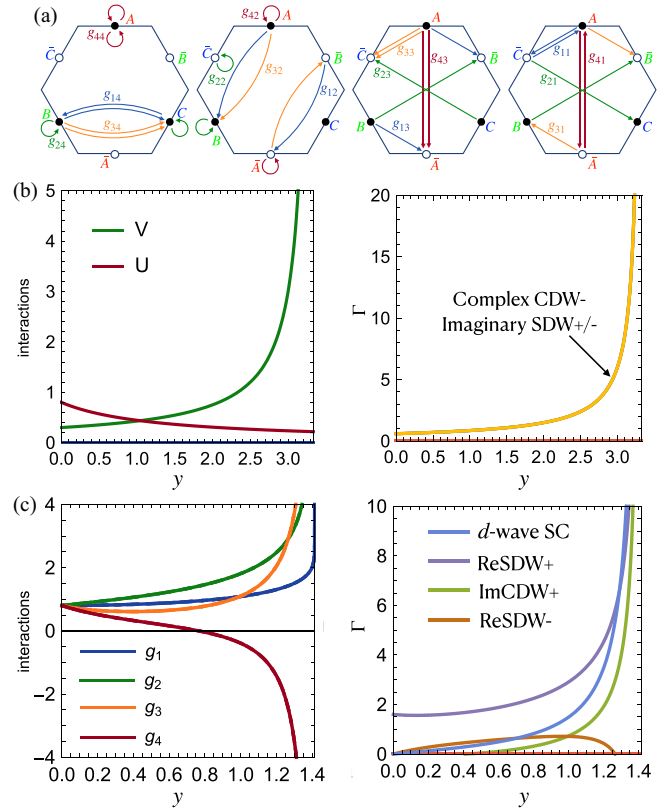

FIG. 2. (a) All symmetry allowed interactions in the six-patch model. (b) RG flow for the interactions and the order parameter vertex Γ with the SI effect. We set $U(0) = 0.8t$ and $V(0) = 0.3t$ and starting from some intermediate energy scale we have $V \gg U$. The resulting weak-coupling instabilities are degenerate complex CDW_- and imaginary $\text{SDW}_{+/-}$. (c) The same RG flow but without SI effect. In this case all the $g_{ij,0}$ are set by the largest Hubbard U, and there does not exist a constant map U, V, and $g_{ij}(y)$. The leading weak-coupling instability is the d-wave SC [35,36].

form $dg_{ij}/dy = g_{mn}R_{mn,kl}g_{kl}$. It is easy to see that close to the critical value y_c all g_{ij} behaves in a similar manner, namely $g_{ij} = G_{ij}/(y_c - y)$. If some G_{ij} is nonzero, the corresponding g_{ij} thus diverges at y_c. A typical order parameter flows as $d\Delta_i/dy = d\Gamma_i\Delta_i$ under renormalization, where $d = 1$ for superconducting orders and $d = d_1 \leqslant \frac{1}{2}$ for density wave orders, and Γ_i is certain linear combination of g_{ij} [39]. From this we can integrate to obtain the behavior of the corresponding susceptibility χ_i, which scales as $\chi_i \sim (y_c - y)^{\gamma_i}$. The leading instabilities will be those with the most negative γ_i, and accordingly the most divergent Γ_i. We mainly consider the following weak-coupling instabilities:

$$\Delta_{\mathrm{CDW}_\pm} = \langle \psi^\dagger_{\alpha+}\psi_{\beta+} \pm \psi^\dagger_{\alpha-}\psi_{\beta-}\rangle,\ \Delta_{\mathrm{SC}} = \langle f_\alpha \psi_{\alpha+}\psi_{\alpha-}\rangle,$$
$$\Delta_{\mathrm{SDW}_\pm} = \langle \psi^\dagger_{\alpha+}\boldsymbol{\sigma}\psi_{\beta+} \pm \psi^\dagger_{\alpha-}\boldsymbol{\sigma}\psi_{\beta-}\rangle. \quad (3)$$

Note that the form factor $f_\alpha = \pm 1$ in Δ_{SC} determines the pairing symmetry. For the density wave orders, their real and imaginary parts flow differently, so depending on whether their imaginary parts are zero or not, the system could either preserve or break the time-reversal symmetry.

In Fig. 2(b) we show the RG results in the presence of SI, i.e., the initial values of g_{ij} are set by Eq. (2). Interestingly, we find that this map between lattice interactions and g_{ij} persists for all $y < y_c$, and it is this constant map that enables us to extract the RG flows for U and V. We see the U decays as before, while V increases. The leading instability in this case is the degenerate complex Δ_{CDW_-} and imaginary $\Delta_{\mathrm{SDW}_\pm}$. The presence of imaginary parts for these density wave orders indicate the time-reversal symmetry is broken [6,41–46], which is due to the SI effect. For comparison, we also show in Fig. 2(c) the RG analysis for the model but with no SI effect. In this case, all g_{ij} are set by the largest interaction U, and the resulting weak-coupling instability is the d-wave uniform superconductivity, consistent with Refs. [35,36].

PDW at intermediate coupling. Having established the way different interactions get renormalized in the presence of the SI effect, we now discuss how the PDW order can emerge at some intermediate energy scale. Based on the observation discussed above [see Fig. 2(b) for example], we consider an effective model where only a large V is kept. Model similar to this has also been studied recently in Ref. [47]. We consider a sufficiently large V, and perform a Hartree-Fock mean-field study [48–52] for the corresponding orders [53]. Without loss of generality, we discuss the AB bond only, as the other bonds follow via C_3 rotation. On the AB bond, the relevant interaction is $2V\cos(\boldsymbol{q}\cdot\boldsymbol{\alpha})\psi^\dagger_{A\sigma}(\boldsymbol{k})\psi^\dagger_{B\sigma'}(\boldsymbol{k}')\psi_{B\sigma'}(\boldsymbol{k}'+\boldsymbol{q})\psi_{A\sigma}(\boldsymbol{k}-\boldsymbol{q})$ where $\boldsymbol{\alpha} = \boldsymbol{a}_1/2$ and $\boldsymbol{a}_1$ is the vector connecting two adjacent A and B sites [see Fig. 1(a)]. Whether this is repulsive or attractive depends on the momentum transfer $\boldsymbol{q}$. In the Cooper channel, we can write it as $2V\cos[(\boldsymbol{k}+\boldsymbol{k}'-\boldsymbol{q})\cdot\boldsymbol{\alpha}]\psi^\dagger_{A\sigma}(\boldsymbol{k})\psi^\dagger_{B\sigma'}(-\boldsymbol{k}+\boldsymbol{q})\psi_{B\sigma'}(\boldsymbol{k}')\psi_{A\sigma}(-\boldsymbol{k}'+\boldsymbol{q})$, which is attractive when $\cos[(\boldsymbol{k}+\boldsymbol{k}'-\boldsymbol{q})\cdot\boldsymbol{\alpha}] < 0$. In the patch model this condition is met when $\boldsymbol{k}$ is around $\boldsymbol{M}_A$, $-\boldsymbol{k}+\boldsymbol{q}$ is around $-\boldsymbol{M}_B$, and $\boldsymbol{k}'$ is around $-\boldsymbol{M}_A$. The interaction then becomes $-2V\psi^\dagger_A\psi^\dagger_{\bar{B}}\psi_B\psi_{\bar{A}}$. When V is large, we can use

$$\psi^\dagger_A\psi^\dagger_{\bar{B}}\psi_B\psi_{\bar{A}} \approx \langle\psi^\dagger_A\psi^\dagger_{\bar{B}}\rangle\psi_B\psi_{\bar{A}} + \psi^\dagger_A\psi^\dagger_{\bar{B}}\langle\psi_B\psi_{\bar{A}}\rangle \quad (4)$$

for mean-field analysis, and the gap function, defined as $\Delta_{\boldsymbol{Q}} \sim \langle\psi_B\psi_{\bar{A}}\rangle$, is apparently a PDW order with momentum $\boldsymbol{M}_C$. We note that due to the presence of SI, the uniform superconductivity is not a competing order in the large V model, since such order couples to, e.g., $\psi^\dagger_A\psi^\dagger_A$, which cannot be obtained by decomposing Eq. (4).

Similarly, the on-site CDW does not arise since this order parameter couples to, e.g., $\psi^\dagger_A\psi_A$, and effectively becomes the chemical potential. However, the bond-charge-density wave (bond CDW) order can indeed arise when V becomes strong [54], and compete with PDW. This occurs also when $\cos(\boldsymbol{q}\cdot\boldsymbol{\alpha}) < 0$ and the density interaction becomes $-2V\psi^\dagger_A\psi^\dagger_{\bar{B}}\psi_B\psi_{\bar{A}}$ with $V > 0$. We can, however, consider

$$-\psi^\dagger_A\psi^\dagger_{\bar{B}}\psi_B\psi_{\bar{A}} \approx \langle\psi^\dagger_A\psi_B\rangle\psi^\dagger_{\bar{B}}\psi_{\bar{A}} + \psi^\dagger_A\psi_B\langle\psi^\dagger_{\bar{B}}\psi_{\bar{A}}\rangle \quad (5)$$

to absorb the minus sign and manifestly show it contains strong repulsion in the particle-hole channel. Moreover, the spin indices on the left-hand side of Eq. (5) can be included explicitly, namely $-\psi^\dagger_{A\alpha}\psi^\dagger_{\bar{B}\beta}\psi_{B\gamma}\psi_{\bar{A}\delta}\delta_{\alpha\delta}\delta_{\beta\gamma}$, and using the $SU(2)$ identity $\delta_{\alpha\delta}\delta_{\beta\gamma} = (\sigma_{\alpha\gamma}\delta_{\beta\delta} + \boldsymbol{\sigma}_{\alpha\gamma}\boldsymbol{\sigma}_{\beta\delta})/2$, it is easy to see that the order parameter $\Delta_{\boldsymbol{Q}} = \langle\psi^\dagger_A\psi_B\rangle$ represents a bond CDW/SDW order, which are directly related to those density waves that arise in the weak-coupling limit. In fact, the degeneracy is an artifact of the oversimplification of the patch model. Considering that the SDW order has to break a global $SU(2)$ symmetry, and upon taking the whole Fermi surface into account, we assume for the time being that the CDW order is more likely to occur than SDW. In the following we thus constrain ourselves to CDW order competing with PDW at large V.

To inspect the competition between PDW and CDW at large $V > 0$, we can calculate the susceptibilities for both of the two orders in random-phase-approximation (RPA). The result is $\chi_{\mathrm{PDW}} = \Pi^0_{pp}(\boldsymbol{Q})/[1 - 2V\Pi^0_{pp}(\boldsymbol{Q})]$ and $\chi_{\mathrm{CDW}} = \Pi^0_{ph}/[1 - 2V\Pi^0_{ph}(\boldsymbol{Q})]$. Here the bare susceptibilities $\Pi^0_{pp} > 0$ and $\Pi_{ph} > 0$ are obtained using free fermion propagators. The ordering condition is given when the denominators vanish. The problem is now reduced to comparing the strength of the bare $\Pi^{(0)}_{pp}$ and $\Pi^{(0)}_{ph}$. Within the patch model, the particle-particle and particle-hole bubbles can be obtained in a straightforward way, and the results are [55]

$$\Pi^{(0)}_{pp}(\boldsymbol{Q}) = \frac{1}{4\sqrt{3}\pi^2 t}\ln\frac{\Lambda}{\max\{T,|\mu|\}},$$
$$\Pi^{(0)}_{ph}(\boldsymbol{Q}) = \frac{1}{8\sqrt{3}\pi^2 t}\ln\frac{\Lambda}{\max\{T,|\mu|\}}\ln\frac{\Lambda}{\max\{T,\mu,|t'|\}}, \quad (6)$$

where $\mu = 0$ at the Van Hove filling, and t' is the next-nearest-neighbor hopping, which can spoil the Fermi surface nesting in the particle-hole channel. In Fig. 3(a) we compare both $\Pi^{(0)}_{pp}$ and $\Pi^{(0)}_{ph}$ as a function of temperature T at $\mu - 0$. We see that the $\ln^2$ divergence of $\Pi^{(0)}_{ph}$ becomes dominant at small T for the case of perfect nesting ($t' = 0$), while at larger T, $\Pi^{(0)}_{pp}$ is larger even with perfect nesting. The consequence is that in the weak-coupling limit, one has to go to small T to see the instability, where CDW wins over PDW. For large V, however, a relatively smaller $\Pi^{(0)}_{pp}$ or $\Pi^{(0)}_{ph}$ is enough to induce the instability, which could be in the regime where $\Pi^{(0)}_{pp} > \Pi^{(0)}_{ph}$ and PDW is the leading instability. Note that Eq. (6) is only a crude estimation about the relative strength between $\Pi^{(0)}_{pp}(\boldsymbol{Q})$

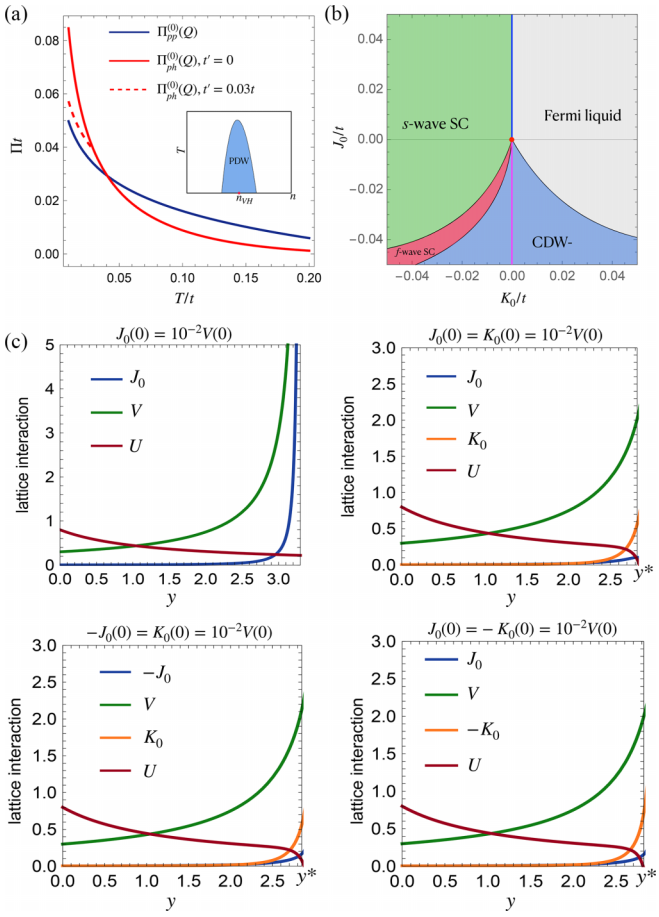

FIG. 3. (a) Comparison between $\Pi^{(0)}_{pp}(\boldsymbol{Q})$ and $\Pi^{(0)}_{ph}(\boldsymbol{Q})$ as a function of temperature T. The fact that $\Pi^{(0)}_{pp}(\boldsymbol{Q}) > \Pi^{(0)}_{ph}(\boldsymbol{Q})$ at larger T indicates that PDW order may win over CDW order when interaction is sufficiently strong. (b) The weak-coupling instabilities (at perfect nesting) when other interactions such as J_0 and K_0 are taken into account. (c) RG flows for the lattice interactions for $U(0) = 0.8t$ and $V(0) = 0.3t$ and for various J_0 and K_0. In all cases there is a wide range in energy scale where V is the largest.

and $\Pi^{(0)}_{ph}(\boldsymbol{Q})$. Away from the Van Hove filling ($\mu \neq 0$), we expect that both bubbles are reduced, and therefore one needs to reach smaller T in order to reach the instability. This results in the schematic picture we show as the inset of Fig. 2(a).

Other interactions. We note that other than U and V, further lattice interaction might be worth analyzing. For instance, we can consider the bond singlet pair-hopping term, for which, again taking AB bond as an example, the on-bond contribution is $J_0 \sum_i P^\dagger_{AB}(\boldsymbol{r}_i) P_{AB}(\boldsymbol{r}_i)$, where the pair operator at position $\boldsymbol{r}_i$ is given by $P^\dagger_{AB}(\boldsymbol{r}_i) = c^\dagger_{A\uparrow}(\boldsymbol{r}_i + \boldsymbol{\alpha}) c^\dagger_{B\downarrow}(\boldsymbol{r}_i) - c^\dagger_{A\downarrow}(\boldsymbol{r}_i + \boldsymbol{\alpha}) c^\dagger_{B\uparrow}(\boldsymbol{r}_i)$ and $\boldsymbol{\alpha} = \boldsymbol{a}_1/2$ is the vector connecting two adjacent A and B sites. In fact, the J_0 term just reads as the exchange interaction. The site pair-hopping term such as $K_0 \sum_{\langle ij \rangle} P^\dagger_i P_j$ with $P^\dagger_i = c^\dagger_{i\uparrow} c^\dagger_{i\downarrow}$ is also possible. With the SI effect, it is easy to realize that J_0 contributes to both g_{1j} and g_{2j}. In particular, $g_{11}(0) = g_{14}(0) = -g_{12}(0) = -g_{13}(0) = 2J_0$, and $-g_{21}(0) = -g_{23}(0) = g_{22}(0) = g_{24}(0) = 2V + 2J_0$. The K_0 term only contributes to g_{3j}: $g_{31}(0) = g_{32}(0) = -g_{33}(0) = -g_{34}(0) = 2K_0$. We expect that J_0 and K_0 are of the same order, and both are orders of magnitudes smaller than U and V [56–59]. In the presence of J_0 and K_0, both of them increase under RG, leading to different orders in the weak-coupling limit, which we present in Fig. 3(b). These include s- and f-wave uniform SC, the real CDW order with odd parity (CDW$_-$). Interestingly, if we keep $K_0 = 0$ there is still a constant map between U, V, J_0, and g_{ij} for all $y < y_c$, and the weak-coupling instabilities are degenerate imaginary $\Delta_{\mathrm{SDW}_\pm}$ for $J_0 > 0$, and a complex Δ_{CDW_-} for $J_0 < 0$ [see the blue and purple line in Fig. 3(b)]. A finite K_0 spoils the constant map between lattice interactions and g_{ij} at y near y_c, but at some intermediate $y^* < y_c$ we can still approximately determine the flow of U, V, J_0, and K_0. Figure 3(c) (see also in [39]) shows that V can still be the largest at intermediate energy scale for various cases, which justifies the applicability of our effective V model discussed above. We close by noting the possibility that when a sizable K_0 is present initially, K_0 could become comparable to V even at $y < y^*$. Since K_0 is related to the formation of uniform SC, and the uniform pairing susceptibility $\Pi^{(0)}_{pp}(0)$ scales as $\ln^2(\Lambda/T)$, one could expect that uniform SC may become leading order. However, in a system with small $K_0(0)$ and thus can be accurately described by the U-V model, our results are applicable.

Discussion. We have focused our analysis entirely on the case of electrons subject to instantaneous repulsive interactions on the kagome lattice near p-type Van Hove filling. At the current level of understanding, it is not yet settled to which extent the kagome metals AV_3Sb_5 (A = K, Cs, Rb) are faithfully represented by this simplified model. Previous attempts to improve on the microscopic rigor by taking into account the multi-orbital nature at the Fermi level [28,60], combined with the relevance of phononic contributions [61], suggest the need for further analysis to quantitatively approach the experimental setup in AV_3Sb_5, and further experiments involving kagome metals are necessary to validate the nature of the CDW observed at scales as high as $T \sim 90$ K . In particular, such order would of course affect the reconstructed bands out of which the superconductivity ultimately develops. A coherent theory of such orders, including the effects of phonons, will only be feasible once the precise nature of the CDW order in this system is well characterized.

Our analysis does, however, make a rare *microscopically founded* statement about the realization of PDW in a physically sensible model, specifically in a kagome metal nearby a p-type vHS with local and nearest-neighbor Coulomb repulsion. This is because SI crucially affects the renormalization of repulsive interactions in kagome metals, and thus the extended repulsive forces are enhanced relative to the on-site Hubbard repulsion. As a result, there is an increased tendency towards PDW and bond CDW order, which we identified without any need for a potentially biased mean-field analysis. Further input from experiment is needed at this stage to bridge the ideas described in this paper with the thus far concluded phase diagram of kagome metals.

Acknowledgements. We sincerely thank Mengxing Ye for useful discussions, and J. Beyer, M. Dürrnagel, T. Müller, J. Potten, and T. Schwemmer for ongoing collaborations on related topics. Y.-M.W. acknowledges the Gordon and Betty Moore Foundation's EPiQS Initiative through Grant

No. GBMF8686 for support at Stanford University. R.T. acknowledges support from the Deutsche Forschungsgemeinschaft (DFG, German Research Foundation) through QUAST FOR 5249-449872909 (Project P3), through Project-ID 258499086-SFB 1170, and from the Würzburg-Dresden Cluster of Excellence on Complexity and Topology in Quantum Matter - ct.qmat Project-ID 390858490-EXC 2147. S.R. is supported by the Department of Energy, Office of Basic Energy Sciences, Division of Materials Sciences and Engineering, under Contract No. DE-AC02-76SF00515.

[1] T.-H. Han, J. S. Helton, S. Chu, D. G. Nocera, J. A. Rodriguez-Rivera, C. Broholm, and Y. S. Lee, Fractionalized excitations in the spin-liquid state of a kagome-lattice antiferromagnet, Nature (London) **492**, 406 (2012).

[2] L. Ye, M. Kang, J. Liu, F. von Cube, C. R. Wicker, T. Suzuki, C. Jozwiak, A. Bostwick, E. Rotenberg, D. C. Bell *et al.*, Massive Dirac fermions in a ferromagnetic kagome metal, Nature (London) **555**, 638 (2018).

[3] M. Kang, L. Ye, S. Fang, J.-S. You, A. Levitan, M. Han, J. I. Facio, C. Jozwiak, A. Bostwick, E. Rotenberg *et al.*, Dirac fermions and flat bands in the ideal kagome metal FeSn, Nat. Mater. **19**, 163 (2020).

[4] J.-X. Yin, W. Ma, T. A. Cochran, X. Xu, S. S. Zhang, H.-J. Tien, N. Shumiya, G. Cheng, K. Jiang, B. Lian *et al.*, Quantum-limit Chern topological magnetism in $TbMn_6Sn_6$, Nature (London) **583**, 533 (2020).

[5] B. R. Ortiz, L. C. Gomes, J. R. Morey, M. Winiarski, M. Bordelon, J. S. Mangum, I. W. H. Oswald, J. A. Rodriguez-Rivera, J. R. Neilson, S. D. Wilson, E. Ertekin, T. M. McQueen, and E. S. Toberer, New kagome prototype materials: discovery of KV_3Sb_5, RbV_3Sb_5, and CsV_3Sb_5, Phys. Rev. Mat. **3**, 094407 (2019).

[6] Y.-X. Jiang, J.-X. Yin, M. M. Denner, N. Shumiya, B. R. Ortiz, G. Xu, Z. Guguchia, J. He, M. S. Hossain, X. Liu *et al.*, Unconventional chiral charge order in kagome superconductor KV_3Sb_5, Nat. Mater. **20**, 1353 (2021).

[7] T. Neupert, M. M. Denner, J.-X. Yin, R. Thomale, and M. Z. Hasan, Charge order and superconductivity in kagome materials, Nat. Phys. **18**, 137 (2022).

[8] H. Chen, H. Yang, B. Hu, Z. Zhao, J. Yuan, Y. Xing, G. Qian, Z. Huang, G. Li, Y. Ye *et al.*, Roton pair density wave in a strong-coupling kagome superconductor, Nature (London) **599**, 222 (2021).

[9] D. F. Agterberg, J. S. Davis, S. D. Edkins, E. Fradkin, D. J. Van Harlingen, S. A. Kivelson, P. A. Lee, L. Radzihovsky, J. M. Tranquada, and Y. Wang, The physics of pair-density waves: Cuprate superconductors and beyond, Annu. Rev. Condens. Matter Phys. **11**, 231 (2020).

[10] E. Fradkin, S. A. Kivelson, and J. M. Tranquada, Colloquium: Theory of intertwined orders in high temperature superconductors, Rev. Mod. Phys. **87**, 457 (2015).

[11] A. Himeda, T. Kato, and M. Ogata, Stripe States with Spatially Oscillating d-Wave Superconductivity in the Two-Dimensional $t - t' - J$ Model, Phys. Rev. Lett. **88**, 117001 (2002).

[12] K.-Y. Yang, W. Q. Chen, T. M. Rice, M. Sigrist, and F.-C. Zhang, Nature of stripes in the generalized t-J model applied to the cuprate superconductors, New J. Phys. **11**, 055053 (2009).

[13] M. Raczkowski, M. Capello, D. Poilblanc, R. Frésard, and A. M. Oleś, Unidirectional d-wave superconducting domains in the two-dimensional $t - j$ model, Phys. Rev. B **76**, 140505(R) (2007).

[14] E. Berg, E. Fradkin, E.-A. Kim, S. A. Kivelson, V. Oganesyan, J. M. Tranquada, and S. C. Zhang, Dynamical Layer Decoupling in a Stripe-Ordered High-T_c Superconductor, Phys. Rev. Lett. **99**, 127003 (2007).

[15] M. Capello, M. Raczkowski, and D. Poilblanc, Stability of RVB hole stripes in high-temperature superconductors, Phys. Rev. B **77**, 224502 (2008).

[16] P. A. Lee, Amperean Pairing and the Pseudogap Phase of Cuprate Superconductors, Phys. Rev. X **4**, 031017 (2014).

[17] Y. Wang, D. F. Agterberg, and A. Chubukov, Coexistence of Charge-Density-Wave and Pair-Density-Wave Orders in Underdoped Cuprates, Phys. Rev. Lett. **114**, 197001 (2015).

[18] Y. Wang, D. F. Agterberg, and A. Chubukov, Interplay between pair- and charge-density-wave orders in underdoped cuprates, Phys. Rev. B **91**, 115103 (2015).

[19] S. D. Edkins, A. Kostin, K. Fujita, A. P. Mackenzie, H. Eisaki, S. Uchida, S. Sachdev, M. J. Lawler, E.-A. Kim, J. C. S. Davis, and M. H. Hamidian, Magnetic field-induced pair density wave state in the cuprate vortex halo, Science **364**, 976 (2019).

[20] Y. Wang, S. D. Edkins, M. H. Hamidian, J. C. Séamus Davis, E. Fradkin, and S. A. Kivelson, Pair density waves in superconducting vortex halos, Phys. Rev. B **97**, 174510 (2018).

[21] Z. Wu, Y.-M. Wu, and F. Wu, Pair density wave and loop current promoted by Van Hove singularities in moiré systems, Phys. Rev. B **107**, 045122 (2023).

[22] Y.-M. Wu, Z. Wu, and H. Yao, Pair-Density-Wave and Chiral Superconductivity in Twisted Bilayer Transition-Metal-Dichalcogenides. Phys. Rev. Lett. **130**, 126001 (2023).

[23] D. Shaffer and L. H. Santos, Triplet pair density wave superconductivity on the π-flux square lattice, Phys. Rev. B **108**, 035135 (2023).

[24] D. Shaffer, F. J. Burnell, and R. M. Fernandes, Weak-coupling theory of pair density-wave instabilities in transition metal dichalcogenides. Phys. Rev. B **107**, 224516 (2023).

[25] J. Ge, P. Wang, Y. Xing, Q. Yin, H. Lei, Z. Wang, and J. Wang, Discovery of charge-4e and charge-6e superconductivity in kagome superconductor CsV_3Sb_5, arXiv:2201.10352.

[26] Y.-M. Wu, P. A. Nosov, A. A. Patel, and S. Raghu, Pair Density Wave Order from Electron Repulsion, Phys. Rev. Lett. **130**, 026001 (2023).

[27] M. L. Kiesel and R. Thomale, Sublattice interference in the kagome Hubbard model, Phys. Rev. B **86**, 121105(R) (2012).

[28] X. Wu, T. Schwemmer, T. Müller, A. Consiglio, G. Sangiovanni, D. Di Sante, Y. Iqbal, W. Hanke, A. P. Schnyder, M. M. Denner, M. H. Fischer, T. Neupert, and R. Thomale, Nature of Unconventional Pairing in the Kagome Superconductors AV_3Sb_5 (A = K, Rb, Cs), Phys. Rev. Lett. **127**, 177001 (2021).

[29] M. Kang, S. Fang, J.-K. Kim, B. R. Ortiz, S. H. Ryu, J. Kim, J. Yoo, G. Sangiovanni, D. Di Sante, B.-G. Park *et al.*, Twofold Van Hove singularity and origin of charge order in topological kagome superconductor CsV_3Sb_5, Nat. Phys. **18**, 301 (2022).

[30] Y. Hu, X. Wu, B. R. Ortiz, S. Ju, X. Han, J. Ma, N. C. Plumb, M. Radovic, R. Thomale, S. D. Wilson *et al.*, Rich nature of Van Hove singularities in kagome superconductor CsV_3Sb_5, Nat. Commun. **13**, 2220 (2022).

[31] I. E. Dzyaloshinskii, Superconducting transitions due to Van Hove singularities in the electron spectrum, Sov. Phys. JETP **66**, 848 (1987).

[32] H. J. Schulz, Superconductivity and antiferromagnetism in the two-dimensional Hubbard model: Scaling theory, Europhys. Lett. **4**, 609 (1987).

[33] H. D. Scammell, J. Ingham, T. Li, and O. P. Sushkov, Chiral excitonic order from twofold Van Hove singularities in kagome metals, Nat. Commun. **14**, 605 (2023).

[34] N. Furukawa, T. M. Rice, and M. Salmhofer, Truncation of a Two-Dimensional Fermi Surface due to Quasiparticle Gap Formation at the Saddle Points, Phys. Rev. Lett. **81**, 3195 (1998).

[35] R. Nandkishore, L. S. Levitov, and A. V. Chubukov, Chiral superconductivity from repulsive interactions in doped graphene, Nat. Phys. **8**, 158 (2012).

[36] R. Nandkishore, R. Thomale, and A. V. Chubukov, Superconductivity from weak repulsion in hexagonal lattice systems, Phys. Rev. B **89**, 144501 (2014).

[37] H. Isobe, N. F. Q. Yuan, and L. Fu, Unconventional Superconductivity and Density Waves in Twisted Bilayer Graphene, Phys. Rev. X **8**, 041041 (2018).

[38] Y.-P. Lin and R. M. Nandkishore, Chiral twist on the high-T_c phase diagram in moiré heterostructures, Phys. Rev. B **100**, 085136 (2019).

[39] See Supplemental Material at http://link.aps.org/supplemental/10.1103/PhysRevB.108.L081117 for i) the sublattice interference is robust against the inclusion of long range hoppings, ii) how the sublattice interference sets the initial values for different patch interactions and iii) the detailed calculation for the bare PDW and CDW susceptibilities.

[40] For comparison, one can also consider the alternative kagome Van Hove filling, which is of *m*-type [see Fig. 1(b)]. There, each ψ_α is a superposition of two distinct lattice fermions and it can be directly verified that the Hubbard U then has equal contributions to all g_i.

[41] L. Yu, C. Wang, Y. Zhang, M. Sander, S. Ni, Z. Lu, S. Ma, Z. Wang, Z. Zhao, H. Chen *et al.*, Evidence of a hidden flux phase in the topological kagome metal, arXiv:2107.10714.

[42] C. Mielke, D. Das, J.-X. Yin, H. Liu, R. Gupta, Y.-X. Jiang, M. Medarde, X. Wu, H. C. Lei, J. Chang *et al.*, Time-reversal symmetry-breaking charge order in a kagome superconductor, Nature (London) **602**, 245 (2022).

[43] X. Feng, K. Jiang, Z. Wang, and J. Hu, Chiral flux phase in the kagome superconductor AV_3Sb_5, Sci. Bull. **66**, 1384 (2021).

[44] Y.-P. Lin and R. M. Nandkishore, Complex charge density waves at Van Hove singularity on hexagonal lattices: Haldane-model phase diagram and potential realization in the kagome metals AV_3Sb_5 (A = K, Rb, Cs), Phys. Rev. B **104**, 045122 (2021).

[45] J.-T. Jin, K. Jiang, H. Yao, and Y. Zhou, Interplay between Pair Density Wave and a Nested Fermi Surface, Phys. Rev. Lett. **129**, 167001 (2022).

[46] T. Park, M. Ye, and L. Balents, Electronic instabilities of kagome metals: Saddle points and Landau theory, Phys. Rev. B **104**, 035142 (2021).

[47] J.-W. Dong, Z. Wang, and S. Zhou, Loop-current charge density wave driven by long-range Coulomb repulsion on the kagomé lattice, Phys. Rev. B **107**, 045127 (2023).

[48] J. Zang, J. Wang, J. Cano, and A. J. Millis, Hartree-Fock study of the moiré Hubbard model for twisted bilayer transition metal dichalcogenides, Phys. Rev. B **104**, 075150 (2021).

[49] C. Repellin, Z. Dong, Y.-H. Zhang, and T. Senthil, Ferromagnetism in Narrow Bands of Moiré Superlattices, Phys. Rev. Lett. **124**, 187601 (2020).

[50] N. C. Hu and A. H. MacDonald, Competing magnetic states in transition metal dichalcogenide moiré materials, Phys. Rev. B **104**, 214403 (2021).

[51] Y. Zhang, K. Jiang, Z. Wang, and F. Zhang, Correlated insulating phases of twisted bilayer graphene at commensurate filling fractions: A Hartree-Fock study, Phys. Rev. B **102**, 035136 (2020).

[52] H. Pan, F. Wu, and S. Das Sarma, Quantum phase diagram of a moiré-Hubbard model, Phys. Rev. B **102**, 201104(R) (2020).

[53] Justification of the Hartree-Fock analysis can be achieved by generalizing the model to a large-N theory, where fluctuations around the saddle point are suppressed by $1/N$ and the Hartree-Fock mean-field equations become asymptotically exact. See [62] and references therein for examples.

[54] M. L. Kiesel, C. Platt, and R. Thomale, Unconventional Fermi Surface Instabilities in the Kagome Hubbard Model, Phys. Rev. Lett. **110**, 126405 (2013).

[55] The apparent dependence on the artificial energy scale Λ is unphysical, and there should be contributions from outside the patches, which eventually add up to make the final results larger and independent of Λ.

[56] J. Hubbard and B. H. Flowers, Electron correlations in narrow energy bands, Proc. R. Soc. London A **276**, 238 (1963).

[57] S. Kivelson, W.-P. Su, J. R. Schrieffer, and A. J. Heeger, Missing Bond-Charge Repulsion in the Extended Hubbard Model: Effects in Polyacetylene, Phys. Rev. Lett. **58**, 1899 (1987).

[58] J. T. Gammel and D. K. Campbell, Comment on the Missing Bond-Charge Repulsion in the Extended Hubbard Model, Phys. Rev. Lett. **60**, 71 (1988).

[59] S. Kivelson, W. P. Su, J. R. Schrieffer, and A. J. Heeger, Kivelson *et al.* Reply, Phys. Rev. Lett. **60**, 72 (1988).

[60] M. M. Denner, R. Thomale, and T. Neupert, Analysis of Charge Order in the Kagome Metal AV_3Sb_5 (A = K, Rb, Cs), Phys. Rev. Lett. **127**, 217601 (2021).

[61] H. Tan, Y. Liu, Z. Wang, and B. Yan, Charge Density Waves and Electronic Properties of Superconducting Kagome Metals, Phys. Rev. Lett. **127**, 046401 (2021).

[62] D. P. Arovas, E. Berg, S. A. Kivelson, and S. Raghu, The Hubbard model, Annu. Rev. Condens. Matter Phys. **13**, 239 (2022).